

High-Efficiency, Fifth-Harmonic Generation of a Joule-Level Neodymium Laser in a Large-Aperture Ammonium Dihydrogen Phosphate Crystal

I. A. Begishev,¹ G. Brent,¹ S. Carey,¹ R. Chapman,¹ I. A. Kulagin,² M. H. Romanofsky,¹ M. J. Shoup III,¹ J. D. Zuegel,¹
and J. Bromage¹

¹Laboratory for Laser Energetics, University of Rochester

²Independent researcher

High-energy deep UV sources are required for high-density plasma diagnostics. The fifth-harmonic generation (5HG) of large-aperture neodymium lasers in ammonium dihydrogen phosphate (ADP) can significantly increase UV energies due to the availability of large ADP crystals. Noncritical phase matching in ADP for ($\omega + 4\omega$) was achieved by cooling a 65×65 -mm crystal in a two-chamber cryostat to 200 K. The cryostat used helium as the thermally conductive medium between the crystal and the internal crystal chamber, which was surrounded by the high-vacuum external chamber with a liquid nitrogen reservoir. A temperature variation of 0.2 K across the crystal aperture was obtained. The total conversion efficiency from the fundamental to the fifth harmonic at 211 nm was 26%.

The higher harmonic provides better penetration of the plasma. An estimated 5ω beam energy of 10 J requires a large-aperture laser and, accordingly, large crystals. Recently we demonstrated a record 5HG efficiency of 30%, producing 335 mJ at 211 nm in a 12×12 -mm beam, using a cesium lithium borate (CLBO) crystal.¹ CLBO has high second-order nonlinearity, can be grown in a relatively large size, and is phase matched at room temperature. Although a CLBO boule could be grown up to $146 \times 132 \times 118$ mm (Ref. 2), practically, the size of a finished optic does not exceed 5 cm. Furthermore, the extremely hygroscopic property of CLBO crystals requires that they be at high temperatures ($\sim 120^\circ\text{C}$). Finally, the cost of manufacturing large CLBO crystals is prohibitive for many applications. ADP crystals, which can be easily grown to much larger sizes, are an alternative way of generating a high-energy beam at 211 nm.

Potassium dihydrogen phosphate (KDP) and ADP crystals are popular nonlinear crystals because of their good nonlinear properties, wide range of transmission, and large sizes. For cascade 5HG, however, they have a significant limitation: phase-matching conditions for sum-frequency generation are not met at room temperature. Noncritical phase-matching conditions could be reached by cooling crystals to -140°C (KDP) and -70°C (ADP). This is not trivial, especially for large-aperture crystals, because a definite temperature must be strictly stabilized and maintained across the entire crystal. Any holder that keeps a crystal in a vacuum chamber and maintains the crystal temperature through thermally conductive contacts provides some temperature gradient across the crystal. The most effective way to stabilize an entire crystal at low temperature is a two-chamber cryostat.³ In our two-chamber cryostat, shown in Fig. 1(a), the tank with liquid nitrogen is connected to the internal chamber through the solid copper (upper) and the hollow stainless-steel (lower) cylinders. The lower hollow cylinder has two 50-W flexible Kapton insulated heaters mounted on the outside surfaces to stabilize the internal chamber temperature. The internal chamber contains the crystal holder with minimized contacts with the crystal to improve the cooling uniformity from the 1 atm of helium that surrounds the crystal. Helium, the main thermal agent between the internal chamber and the crystal, was chosen because of its high (compared with other gases) thermal conductivity. Three silicon diode cryostat temperature sensors are located on two outside points of the internal chamber and on one side of the crystal inside the internal chamber. Two 120-mm-diam, 10-mm-thick fused-silica windows are located on opposite sides of the internal chamber coaxially to the crystal to pass input and output beams.

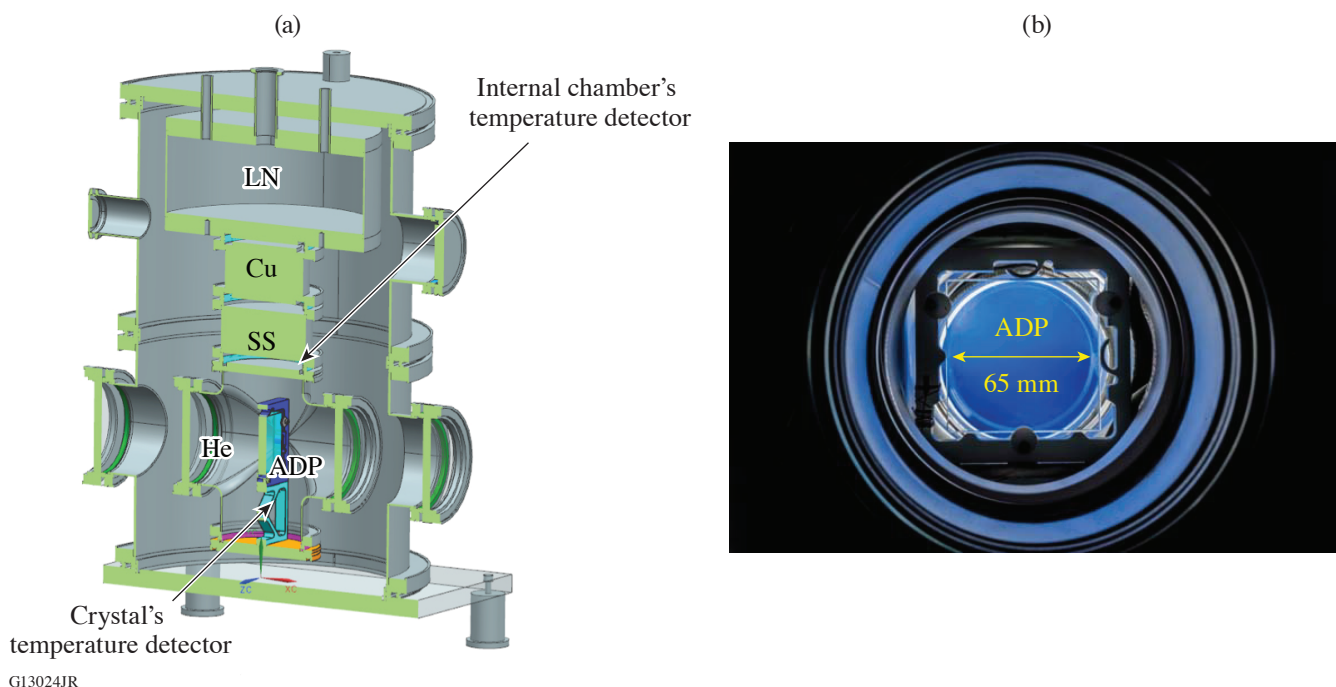


Figure 1

(a) The cross section of the two-chamber cryostat with the liquid nitrogen tank (LN), the copper cylinder (Cu), the stainless-steel cylinder (SS), and the internal chamber filled with helium (He) with an ADP crystal inside; (b) a photo of an ADP crystal inside the two-chamber cryostat through two input windows.

“Cold flow” goes down from the liquid nitrogen tank to the internal chamber; it then reaches the crystal through the helium. As soon as the temperature of the crystal reaches a chosen set point temperature, the heaters begin working to maintain that temperature through a temperature-stabilization loop with 0.01°C resolution controlled by a proportional integral derivative feedback loop. The feedback continually adjusts the output power to the heaters in order to keep the chosen temperature constant. The system has high thermal mass and reaches the target 200 K temperature in about 36 h.

The internal chamber is installed into the external chamber, which is pumped down to a vacuum of better than 5×10^{-7} Torr. The external chamber also has input and output windows, so the two-chamber cryostat has a total of four windows. The two input windows have sol-gel antireflection (AR) coatings at 266 nm (4ω), while the output windows are coated at 211 nm (5ω). The ADP crystal ($65 \times 65 \times 10$ mm, type I, $\theta = 90^{\circ}$, $\phi = 45^{\circ}$) has AR coatings at 1ω and 4ω on the input face and an uncoated output face.

A special heavy-duty rotation stage was designed and fabricated to carry this large, heavy two-chamber cryostat and rotate it within an angular range of 5° with microradian accuracy. As a result, phase matching could be tuned by both crystal temperature and angle.

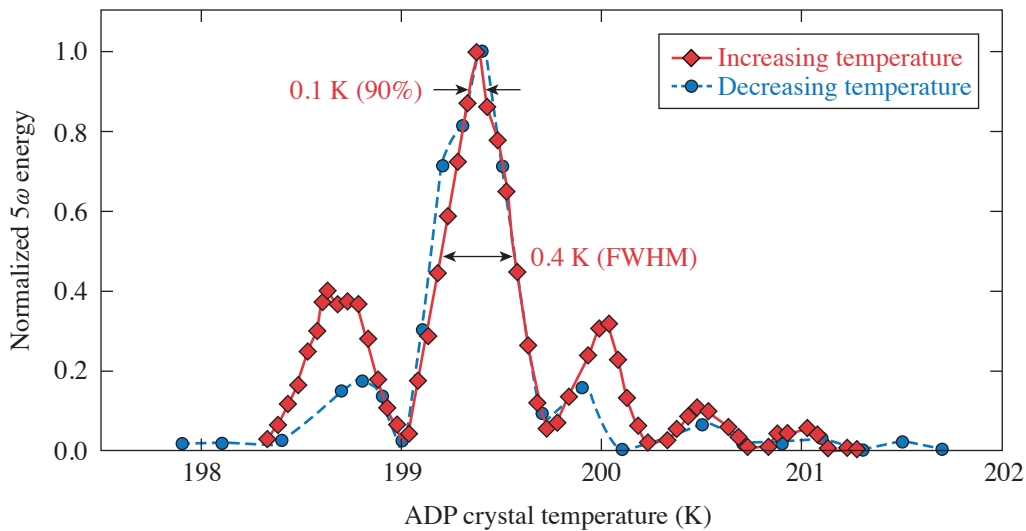
The thermal model was developed based on COMSOL Multiphysics[®] and was able to predict the lowest-reachable temperature of 170 K and the cooling time to reach that temperature.

There are two possible frequency-conversion schemes to optimize 5HG in a cascade of three nonlinear crystals, remembering that no type-II phase matching for 4HG (fourth-harmonic generation) and 5HG exists in KDP and ADP: $o_1o_1 \rightarrow e_2:o_2o_2 \rightarrow e_4:o_1o_4 \rightarrow e_5$ and $o_1e_1 \rightarrow e_2:o_2o_2 \rightarrow e_4:o_1o_4 \rightarrow e_5$, where o and e are ordinary and extraordinary waves in crystals. In the first case, we must detune sum-harmonic generation (SHG) down from the maximum by adjusting the length of the first crystal, while two

other processes (4HG and 5HG) should be maximized. In the second case, the required energy distribution between orthogonal polarizations could be set by rotating the input beam polarization. Here the energy distribution is adjustable for any given input energy, making the second case preferable.

The angle α between input-beam polarization and the horizontal plane was tuned by a half- λ wave plate in front of the first crystal. It changes the balance of energy between the ordinary and extraordinary axes in the first type-II doubler and preserves some fraction of the fundamental frequency beam through the first two crystals for the interaction in the last crystal. The first frequency doubler was a deuterated potassium dihydrogen phosphate (DKDP) crystal ($30 \times 30 \times 27$ mm), which was chosen instead of KDP to decrease linear absorption at the fundamental frequency. It was cut in a type-II configuration to convert $1\omega \rightarrow 2\omega$. A second frequency doubler, a type-I KDP crystal ($30 \times 30 \times 15.5$ mm), was used to convert $2\omega \rightarrow 4\omega$. The final crystal, made of ADP, was located at the image plane of a Nd:YLF laser⁴ that was optimized to produce a flattopped, square-beam profile with a square pulse (1053 nm, 12×12 mm, from 1 ns to 2.8 ns, ≤ 1.5 J, 5 Hz, 0.1 Hz, or a single shot). A fused-silica prism separates the harmonic beams in space. The input and output beam energies were measured using identical cross-calibrated pyroelectric energy meters.

We reached 5HG at -73°C (200 K). The temperature acceptance of 5HG in ADP at a fixed crystal angle was measured (see Fig. 2). Each point was taken without temperature stabilization at a given temperature: 5ω energy was measured while the temperature of the ADP crystal was slowly drifting. “Red” data were taken while the crystal temperature was increasing, and “blue” data were taken while crystal temperature was decreasing. Note that the red curve was shifted down by 0.07 K to match the blue curve. This difference likely comes from the temperature gradient without stabilization and system lag because of the thermal mass.



E28202JR

Figure 2

Fifth-harmonic energy temperature (T) acceptance at a fixed position angle of the ADP crystal.

An important point here is that the temperature acceptance is only 0.4 K (FWHM). To keep the system close to the maximum (>90%) of 5HG efficiency, an ADP crystal must be temperature stabilized with an accuracy better than 0.1 K. Figure 3 shows beam profiles of the input beam at the fundamental frequency (a) before the first crystals and (b) fifth-harmonic beam after the cryostat. Compared to the relatively uniform 1ω beam, the 5ω beam is slightly more spatially varied. Some residual radial nonuniformity of the 5ω beam was caused by a small phase mismatch inside the ADP crystal and corresponds to a temperature gradient over the ADP crystal. Overall conversion efficiency could be better with improved temperature uniformity of the ADP crystal.

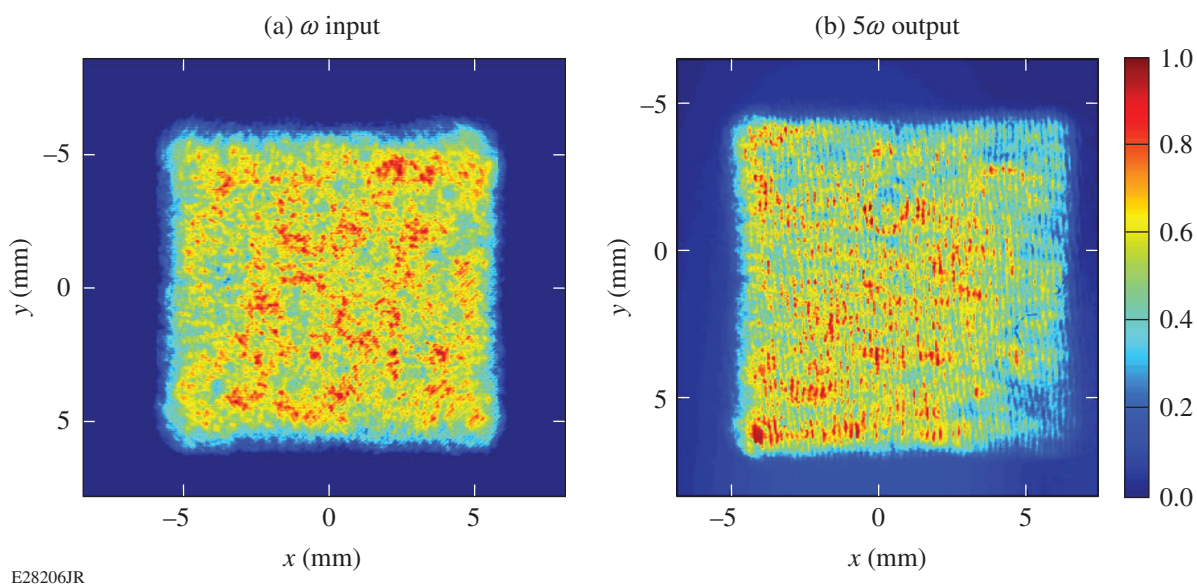


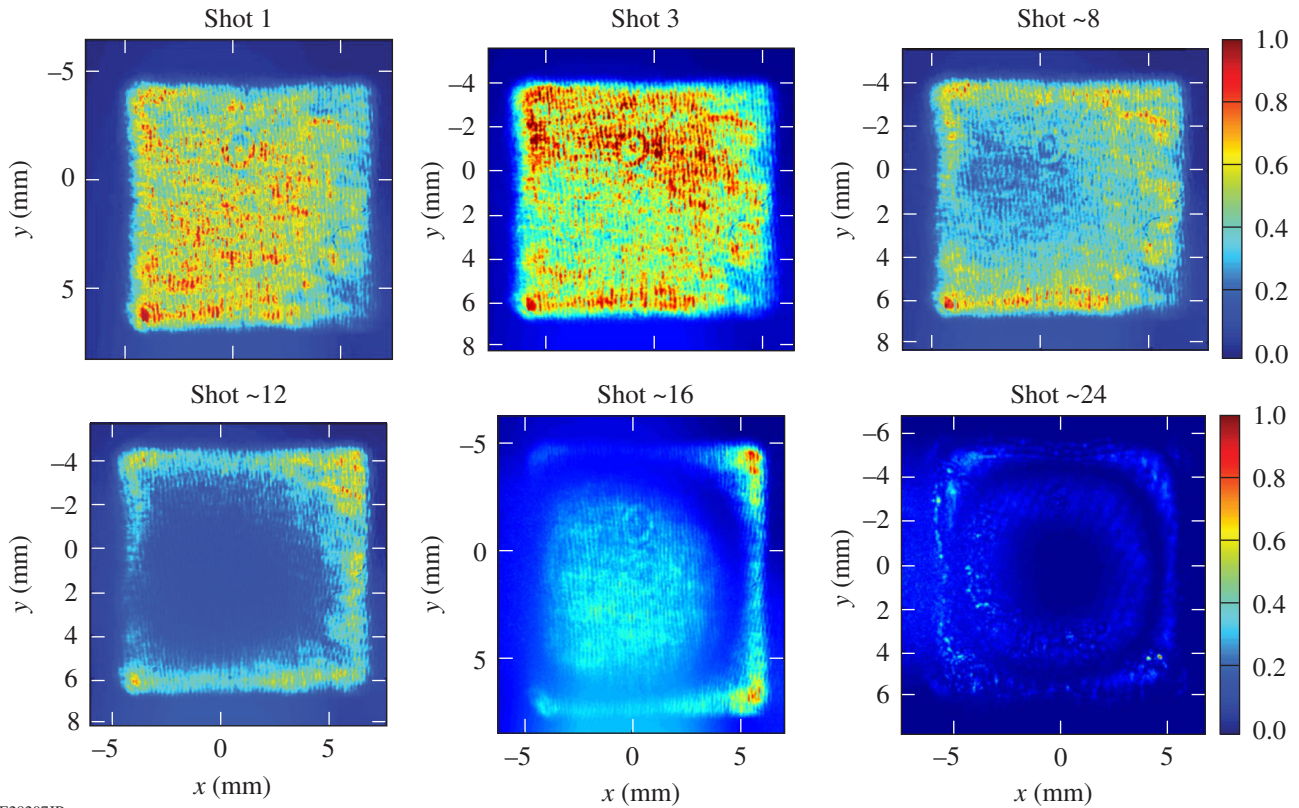
Figure 3

Input beam image (a) at the fundamental frequency on the front of the cascade of crystals and fifth-harmonic output beam image (b) after the cryostat.

Because the ADP crystal is isolated in a helium atmosphere with very low direct conductivity to the chamber, even a small amount of energy absorption from the interaction laser beams cannot be rapidly dissipated. As a result, the ADP and other crystals in a gas cryostat work well in a single-shot regime (about one shot per minute) but cannot work at a high repetition rate because of phase mismatch caused by laser heating. Figure 4 shows the sequence of fifth-harmonic output beam images behind the cryostat taken after a various number of shots running at a 5-Hz repetition rate. Even a small amount of absorbed laser energy inside a crystal after the first shot makes the crystal warmer in the center and disturbs the temperature distribution, resulting in a spatially varying phase mismatch that grows as a series of radial rings. The 5ω beam almost disappears after 24 shots. This effect is negligible provided there is sufficient time for the crystal to thermalize. A one-minute interval between shots is enough to maintain the required temperature distribution of 0.1 K over the crystal aperture.

The angular acceptance of 5HG at a given temperature of the ADP crystal was measured as 8 mrad external (FWHM). After careful optimization, the 5HG efficiency became as high as 26% at a 0.1-Hz repetition rate with a 2.4-ns pulse and an input intensity of 0.3 GW/cm^2 . This efficiency describes the portion of the input 1ω energy that has been transformed into the fifth harmonic and is available at the output of the cascade of crystals for use in any application, and includes linear and nonlinear loss mechanisms.

The energy balance is the ratio of the total energy of all beams after the cryostat to the 1ω energy at the input of the first crystal of the cascade. Therefore, it represents a fraction of energy transmitted from input to output through all three crystals and the cryostat. The initial balance is just 62% at very low input beam intensity and corresponds to passive losses, mostly coming from linear absorption and Fresnel reflections. It also demonstrates that the total conversion efficiency of 5HG could be increased by, for example, better AR coatings and crystalline windows. At high input beam intensity the total energy transmitted through the system and the energy balance drop due to significant nonlinear losses, which dramatically limits 5ω conversion efficiency. The energy balance at peak 5HG efficiency was 48%, with the additional losses coming mainly from two-photon absorption (TPA). We measured TPA at 211 nm in air (13.5 m) and in the longer (15-mm) ADP crystal cut at the x plane using the 5ω beam from the above-described setup. The TPA coefficient of ADP at 211 nm was measured as $(1.2 \pm 0.2) \text{ cm/GW}$. Due to a relatively small dynamic range of the input energy, that measurement is not very accurate. The difference in TPA's of ADP along different crystal axes is within the error of the measurement. We also measured TPA in the air ($0.0008 \pm 0.0002 \text{ cm/GW}$) and in fused silica ($0.5 \pm 0.1 \text{ cm/GW}$) at 211 nm and in ADP at 263 nm ($0.25 \pm 0.1 \text{ cm/GW}$).



E28207JR

Figure 4
Fifth-harmonic output beam images after the cryostat taken after a various number of shots running at a 5-Hz repetition rate.

The authors thank S. Yang, P. Datte, and S. Patankar at Lawrence Livermore National Laboratory for the support and helpful discussions. This material is based upon work supported by the Department of Energy National Nuclear Security Administration under Award Number DE-NA0003856, the University of Rochester, and the New York State Energy Research and Development Authority.

1. I. A. Begishev *et al.*, *Opt. Lett.* **43**, 2462 (2018).
2. X. Yuan *et al.*, *J. Cryst. Growth* **293**, 97 (2006).
3. I. A. Begishev *et al.*, *J. Appl. Spectrosc.* **51**, 1218 (1989).
4. V. Bagnoud *et al.*, *Appl. Opt.* **44**, 282 (2005).